ADVANCED MATERIALS
www.advmat.de

The Design of a Heterocellular 3D Architecture and its Application to Monitoring the Behavior of Cancer Cells in Response to the Spatial Distribution of Endothelial Cells

Wonjae Lee and Jon Park**

Since most biological phenomena involve orchestration of multiple cellular interactions, the spatial cell distribution is one of the critical features for governing cell behaviors.[1] There have been attempts to regulate cell distribution with microfluidic patterning,[2] microgel,[3] photolithographic patterning,[4] electrophoresis,[5] and 3D printing.[6] Tissue-engineering strategies have opened the possibility of in vitro monitoring of various biological processes in more-natural 3D conditions by recapitulating key aspects of the original tissue microenvironments and structures.[7] Hydrogels have been successfully utilized as a scaffold material of engineered tissues to provide 3D environments that are biophysically similar to human extracellular matrices and to restore in vivo behaviors of the incorporated cells that were lost in traditional 2D cultures.[8] However, it has been a challenge to construct hierarchical multicellular 3D engineered tissues within hydrogel-based scaffolds while eliciting reliable heterotypic cellular interactions. In this work, we suggest a novel method of building a hierarchical cellular structure by stacking cell-attached microplate structures with specific configurations within hydrogel layers. The plate structures were prepared by aggregation of poly(lactide-co-glycolide) (PLGA) particles on a microstructured mold. We first verified that, by reconstructing the 3D architecture of a liver lobule, our method maintained cell viability while providing a favorable environment for heterotypic cellular interaction resulting in improved tissue function. This method was then utilized to construct an engineered tumor to monitor and modulate cancer-cell behaviors in response to the spatial distribution of neighboring endothelial cells. The interaction between the cancer cells and the endothelial cells is of importance in investigating the physiological complexity underlying cancer growth and developing more-advanced chemotherapeutic strategies.[9] Their interaction is characterized by formation of new blood vessels sprouting toward the neighboring tumors with three major purposes: to support the metabolic activities of tumors for further growth, to enable the invasion of cancer cells through the formed blood vessels for metastasis, and to facilitate paracrine stimulations for cancer cells against apoptosis.[9–11] Our approach successfully granted the engineered tumors the behaviors resembling the initial phases of cancer angiogenesis and invasion. Furthermore, our engineered tumors showed a higher resistance to several chemotherapy drugs compared with cancer cells cultured in traditional 3D systems. We expect this method holds promise for the development of in vitro experimental models to elucidate the role of heterocellular interactions in various biological phenomena.

We first developed microplate structures with specific configurations. By attaching endothelial cells onto these plate structures we could maintain specific configuration of the cell distribution and thus ensure their stable homotypic cellular interactions required for angiogenesis.[12] We also designed the plate structures such that they would provide enough contact faces to other cells types and that they would be fit for the local deliverance of drugs like vascular endothelial growth factors (VEGF) to promote the formation of new blood vessels. We selected PLGA for the structure material because the strategies for incorporating drugs in PLGA and controlling the drug releasing rates have been well-determined.[13] We constructed the plate structures by shaping a microstructured mold and then aggregating VEGF-encapsulating particles into it (**Figure 1**a). Using the fully cured particles granted more-reliable control over casting the polymer into the micrometer-scale depressions of the mold than using the polymer solution itself. The particles were prepared by a water-in-oil-in-water (w/o/w) method. The w/o/w method employs the immiscibility between a drug-containing aqueous solution and a nonpolar polymer solution for isolating drug-containing droplets and encapsulating them within the polymer matrix of the particles without compensating the drug efficacy.[13] In order for the encapsulated VEGF to be safely translated into the microplate structures, we aggregated the particles before the VEGF-containing droplets dried out. This process enabled the plate structure to retain the porosity of the aggregated particles (Figure 1b). We confirmed that there was no statistical difference in the drug activity (Figure 1c) and the encapsulation efficiencies (Supporting Information, Figure S1) between the free particles and the plate structures. We also observed that the plate structures had a decreased initial burst of the released VEGF compared with the free particles (Figure 1d). This is beneficial to clinical efficacy because the initial burst implies the risk of exceeding the toxic limits and hinders the regulation of the drug-releasing rate for optimal deliverance.[13] Since the configuration of the drug-releasing plate structure could be easily modified by the shape of a polydimethylsiloxane (PDMS) mold, this approach

W. Lee, J. Park
Department of Neurosurgery
Stanford University
300 Pasteur Drive, Stanford, CA 94305
USA Stanford, CA, USA
E-mail: wjh@stanford.edu; jonpark1@stanford.edu
Dr. W. Lee, Prof. J. Park
Department of Neurosurgery
Stanford University
300 Pasteur Drive, Stanford, CA 94305, USA

DOI: 10.1002/adma.201200687

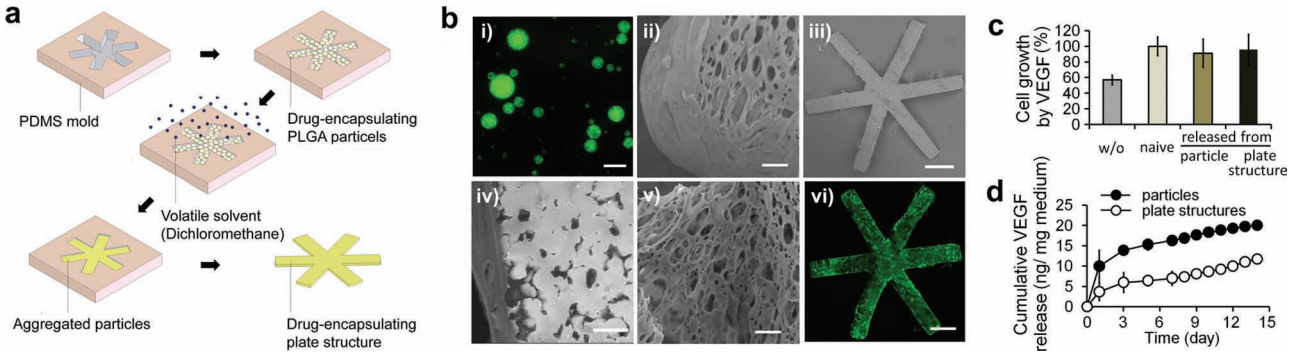

Figure 1. a) Schematic illustration of the preparation of a drug-encapsulating plate structure. b) For presentation purposes, fluorescein isothiocyanate-conjugated bovine serum albumin (FITC-BSA) was used in these images instead of VEGF: i) Fluorescent image of the FITC-BSA-encapsulating particles (scale bar: 20 μm); ii) Scanning electron microscopy (SEM) image of a cross section of a particle prepared from the water-in-oil-in-water emulsion (scale bar: 2 μm); iii) SEM image of the overall shape of a microplate structure (scale bar: 300 μm); iv) SEM image of the surface of a microplate structure (scale bar: 30 μm). v) SEM image of a cross section of a plate structure (scale bar: 2 μm); vi) fluorescent image of the plate structure prepared with FITC-BSA-encapsulating particles (scale bar: 300 μm). c) The biological activity of VEGF was determined by its mitogenic activity on HUVEC at 10 ng/mL concentration. We prepared different sample groups; HUVEC cultured without VEGF (denoted as 'w/o), with fresh VEGF (denoted as 'naïve'), with released VEGF from free particles and from plate structures respectively. There was no activity change through the overall preparation process (i.e., no changes across the latter three groups ($n = 2$, $p > 0.01$)). d) The VEGF-releasing profiles from plate structures and from free PLGA particles ($n = 3$). One plate structure weighs about 0.3 mg.

has potential to be utilized in generating specific spatial gradients of many other biologically active molecules.

To test our approach as a valid in vitro model system for monitoring heterocellular interactions, we applied it to construct a spatial mimic of a highly vascularized liver lobule, the structural unit of the liver. We chose the liver lobule because, in addition to all the significances of the liver function to human body, the interactions of hepatocytes with non-parenchymal cells, such as endothelial cells, could be easily evaluated by the secretion amount of hepatic function markers.[14] **Figure 2**a describes the procedure to construct the key architectural features of the liver lobule using human hepatocytes and human umbilical vein endothelial cells (HUVEC). The cross-sectional views of the engineered liver lobule are shown in Figure 2b. In order to isolate the effect of VEGF as a mitogen, we first prepared the engineered tissues with plate structures without VEGF. The overall construction process did not have any negative influence on hepatocyte viabilities (Figure 2c). We used urea as a surrogate marker for overall functions of the encapsulated hepatocytes since its molecular dimension is small enough not to be trapped by a hydrogel network.[14] The hepatocytes in the engineered lobules showed increased urea secretion compared with the hepatocytes encapsulated in plain hydrogel matrices or co-encapsulated with HUVEC without any pattern (Figure 2d). The coculture with the same ratio in a traditional 2D culture did not show any significant improvement (Figure S2). This is because the favorable spatial distribution for

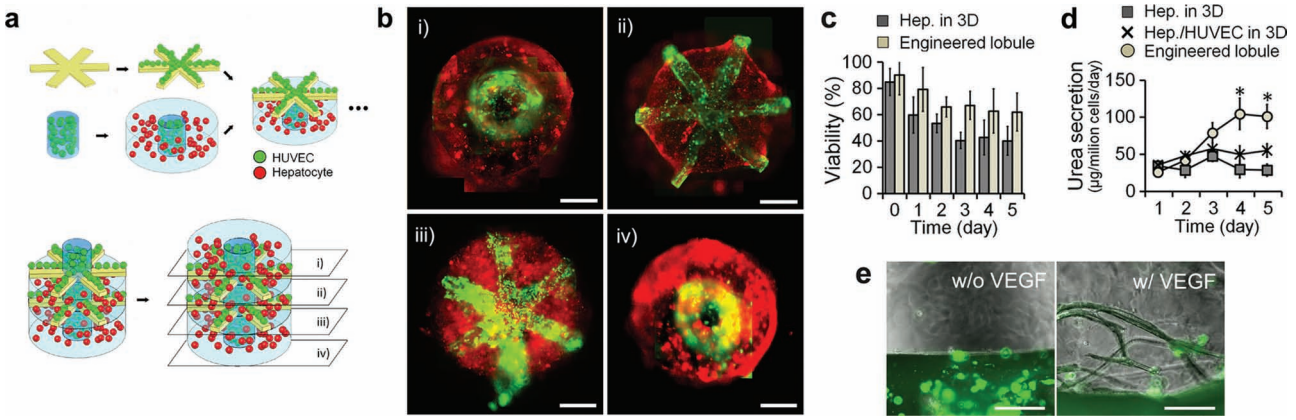

Figure 2. a) Schematic illustration of constructing the liver-lobule architecture. HUVEC were loaded on plate structures which in turn were layered between hepatocyte-containing hydrogel layers. b) Cross-sectional fluorescent images of the engineered liver lobule. Hepatocytes and HUVEC were prestained as red and green, respectively (scale bar: 300 μm). c) The viability of hepatocytes in the engineered liver lobules did not show a statistical difference compared with their viability in plain 3D hydrogel matrices (denoted as 'Hep. in 3D') ($n = 3$, $p > 0.01$). d) Urea secretion as a hepatic function marker was measured in three sample groups; hepatocytes encapsulated in 3D hydrogel matrices ('Hep. In 3D'), cocultured with HUVEC in 3D hydrogel matrices ('Hep./HUVEC in 3D'), and in engineered liver lobules. Four days after encapsulation, there were statistically significant increases in the engineered liver lobules compared with the other two sample groups ($n = 3$, statistical significances are denoted as asterisks when $p < 0.01$). e) When VEGF-containing plate structures were incorporated with HUVEC (prestained as green), the cells migrated and aligned only around the plate structures (scale bar: 100 μm). The hepatocytes are not coencapsulated in these pictures for visual clarity.

both homotypic and heterotypic cellular interactions in our engineered liver lobule promoted hepatic functions.[14] When VEGF-encapsulating plate structures were incorporated, there was an increase in the amount of urea secretion (Figure S3), demonstrating the encapsulated VEGF were delivered intact to the hepatocytes. In addition, we also observed the migration and alignment of endothelial cells only within the plate structure (Figure 2e). (Due to the lack of direct verification of the epithelium basement membranes and the tubular configuration in our experimental results, we limited the description of the similar cell behaviors observed in this study to the migration and alignment of endothelial cells.) The localized migration implies that our method can provide more-reliable control over the spatial distribution of the newly formed capillaries compared with the approaches based solely on releasing angiogenic factors or seeding endothelial cells without any specific configuration which can only induce non-directional formation of capillary structures.

We applied this method to construct an in vitro platform for monitoring the interactions of cancer cells with endothelial cells. In the following experiments, the plate structures had no encapsulated drug. We first prepared L-shaped plate structures in the same way as described in Figure 1a. The plate structure with attached HUVEC was laid out within the outskirt of the hydrogel matrix and a cluster of cancer cells (C6 rat glioma) was placed in the center (Figure 3a). This lay-out was intended to spatially mimic the initial phase of a tumor before vascularization. We also optimized the thickness of the hydrogel matrix (1 mm) to limit the diffusion of indispensable substances, especially oxygen, to generate hypoxic state so that the expression of VEGF, one of the key regulatory factors for cancer angiogenesis, could be upregulated in the incorporated cancer cells (Figure S4). Three days after cell encapsulation, we observed the alignment of migrating endothelial cells sprouting toward the cancer-cell colony and penetrating it (**Figure 3**a(i)). Figure 3a(ii)

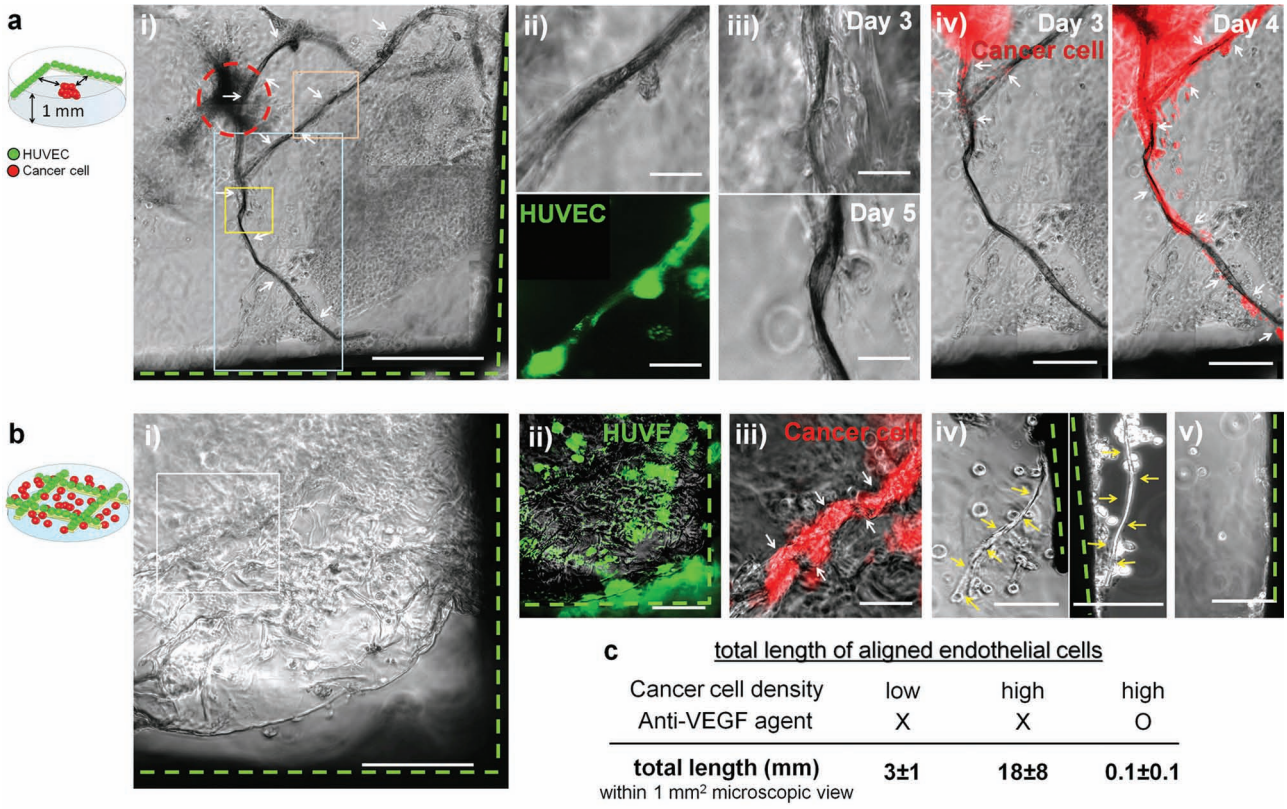

Figure 3. The green and red dashed lines represent the HUVEC (prestained as green)-attached microplate structures and the positions where the cancer cells (prestained as red) were loaded, respectively. No drug was incorporated into these plate structures. a) Cancer cells (C6 rat glioma) and HUVEC were laid out to spatially mimic the initial phase of the cancer development (see the upper left illustration): i) three days after cell encapsulation, the endothelial cells migrated and aligned toward the cancer-cell colony (white arrows) (scale bar: 500 μm); ii) the magnified images of the orange box in Figure 3a(i) showing HUVEC migration (scale bar: 30 μm); iii) the magnified optical images of the yellow box of Figure 3a(i) showing the configuration of the cell alignments matured to have a solid layer. (scale bar: 30 μm); iv) a merged image of the blue box of Figure 3a(i) with the fluorescent image of the cancer cells. After the alignment of migrating endothelial cells penetrated the cancer-cell colony, the cancer cells migrated along the aligned HUVEC (scale bar: 150 μm). b) Cancer cells and HUVEC were located to spatially mimic highly vascularized tumors (see the upper left illustration): i) optical image of the engineered tumor with a cross-shaped plate structure on which HUVEC were initially located. Around the highly dense cancer cells (initially encapsulated at 40×10^6 cell/mL), numerous uneven luminal layers of the HUVEC alignments were observed (scale bar: 200 μm); ii) fluorescent image of Figure 3b(i) where HUVEC migrated from the plate structure (scale bar: 200 μm); iii) magnified image of the white box in Figure 3b(i), merged with the fluorescent image of the cancer cells. Cancer cells migrated along the HUVEC alignment (scale bar: 50 μm); iv) migration of HUVEC (yellow arrows) was reduced in the engineered tumor with a low density of cancer cells (initially encapsulated at 1×10^5 cell/mL, scale bar: 100 μm); v) No migration of HUVEC was observed when HUVEC-attached plate structures were not incorporated with cancer cells (scale bar: 100 μm). c) The lengths of the aligned endothelial cells were determined based on the analysis of the optical-microscopic views (1 mm × 1 mm).

shows that these alignments were formed by the migration of HUVEC that had been initially located on the plate structure. Since the cancer cells in hypoxia release an angiogenic factor, VEGF, the endothelial cells in neighboring blood vessels sprout new blood vessels toward the angiogenic stimuli (i.e., the cancer cells).[15] This endothelial cell migration is the initial step for cancer angiogenesis and is followed by lumen formation for further vasculature maturation.[16] We also observed that they matured to have more solid layers (Figure 3a(iii)). Once the alignment of the migrating endothelial cells penetrated the cancer-cell colony, we observed that the cancer cells migrated along the aligned HUVEC as well (Figure 3a(iv) and Figure S5). These results demonstrate that our engineered tumors successfully provided the proper environment to induce the cancer-cell behaviors recapitulating the hallmarks of in vivo cancer development, angiogenesis and invasion.[17]

We next developed engineered tissues that spatially imitated a highly vascularized mature tumor by utilizing a cross-shaped plate structure (Figure 3b). Three days after cell encapsulation, we observed the alignments and the migration of HUVEC (Figure 3b(i), (ii) and Figure S6). The configuration of the cell alignment was similar to the morphology of in vivo tumor vasculatures, where they have uneven luminal layers and show loss of vessel hierarchy.[12] This morphology is in stark contrast to the morphology showing even luminal layers induced by VEGF alone without neighboring cancer cells (Figure 2e). We also observed the migration of cancer cells within the endothelial cell alignments (Figure 3b(iii)). The engineered tumor with low density cancer cells showed reduced migration of the endothelial cells (Figure 3b(iv) and Figure 3c). All these behaviors of HUVEC are in marked contrast to when HUVEC were incorporated without cancer cells (Figure 3b(v)). Because VEGF is one of the major angiogenic stimuli induced by cancer cells,[15] we incorporated anti-VEGF agents (bevacizumab) to suppress the interactions between the two types of cells. As we expected, there was reduced migration of endothelial cells (Figure 3c). These results suggest that the observed cell behaviors in the engineered tumors were mainly mediated by VEGF and induced by the interaction of the incorporated cancer cells with the neighboring endothelial cells.

Based on these results, we hypothesized that our approach could offer a more clinically relevant in vitro platform for monitoring cancer-cell apoptosis by chemotherapy, because most of the current chemotherapy drugs kill cancer cells by apoptosis whereas the endothelial cells on tumor vasculatures work as paracrine stimulators for cancer cells against apoptosis.[18] To test it, we prepared highly vascularized engineered tumors as shown in Figure 3b and incubated them in the cell culture medium with three different classes of chemotherapy drugs; paclitaxel, curcumin and mitomycin C. Paclitaxel interacts with polymerized tubulin to promote the formation of microtubules and to prevent their disassembly so that it can have selective cytotoxicity to rapidly dividing cells. Curcumin causes cytotoxicity to cancer cells by its downregulation effect on the transcription nuclear factor-κB (NF-κB), which is linked with proliferation, invasion, and angiogenesis as well as suppression of apoptosis. Mitomycin C is a bioreductive alkylating agent and preferentially activated by cancer cells in hypoxic state. The cancer-cell responses to these drugs in our engineered tumors were compared with the responses of the cancer cells co-encapsulated with randomly distributed HUVEC. We found that our engineered tumors conferred a higher level of resistance to all three drugs (**Figure 4**i, ii, and iii). This is in line with the previous works reporting that the resistance to chemotherapy drugs mainly arises in highly vascularized mature tumors.[19] Importantly, the incorporation of the anti-VEGF agents increased drug efficacy (Figure 4iv, v, and vi), which corresponds to clinical data.[11] These data suggest that in order to monitor the cancer-cell apoptosis or chemotherapy drug efficacies in a more-natural, clinically relevant environment, the ability to induce reliable heterocellular interactions between cancer cells and endothelial cells is critical. It was made possible in our engineered tumors by modulating the 3D spatial configurations of the two cell types.

Even though our engineered tissues did not incorporate the complete set of the in vivo physiological conditions, they successfully recapitulated the key aspects of the native tissue structures for reliable heterocellular interactions, proven by the restored in vivo behaviors of the incorporated cells. We believe our method laid the groundwork for developing more-advanced, hydrogel-based 3D engineered tissues in which the holistic structure and the function of hierarchical multicellular organizations could be reconstructed for elucidating the role of the interactions between different types of cells in various biological phenomena.

Experimental Section

Preparation of PLGA Microplate Structures: Microstructures were prepared in silicon wafers using standard microfabrication processing techniques and transferred to a PDMS replica. The etch thickness was targeted to be 150 μm. On the surface of the PDMS mold, fully cured PLGA particles (see "Additional Materials and Methods" in the Supporting Information) were loaded and spread so that the particles could be evenly filled into the micro-structured depressions of the mold. They were then incubated in a covered glass Petri dish with small amount of dichloromethane (DCM) at 37 °C for 15 min so that the evaporated DCM could promote particle aggregation by being adsorbed on the surfaces. To keep the encapsulated VEGF isolated during the aggregation process, we completed the aggregation process before the VEGF-containing droplets dried out from the particles. The aggregated particles were left at room temperature for 30 min for the structure to be stabilized and then removed using a dissection microscope.

Construction of Three-Dimensional Engineered Tissues: Dried microplate structures were drenched into 70% ethanol and washed with an excess amount of phosphate buffered saline (PBS). For cells to be easily attached, the structures were soaked with fetal bovine serum (FBS) for 10 min and left in a vacuum desiccator overnight. Then they were loaded on an ultralow attachment surface culture dish (Corning) and covered with a HUVEC suspension for three hours until the endothelial cells were attached. Our engineered tissues were developed based on matrix-metalloproteinase (MMP)-sensitive hydrogels that have been reported to enable cell invasion and lead to tissue regeneration.[20] We utilized commercially available poly(ethylene glycol) (PEG)-based hydrogels (QGel, QGel SA) with MMP-sensitive substrates and cell-adhesion domains.

To construct the 3D structure of the engineered liver lobule, we first cured 0.3 μL of hydrogel prepolymer with HUVEC between two glass slides separated by a polytetrafluoroethylene (Teflon) spacer

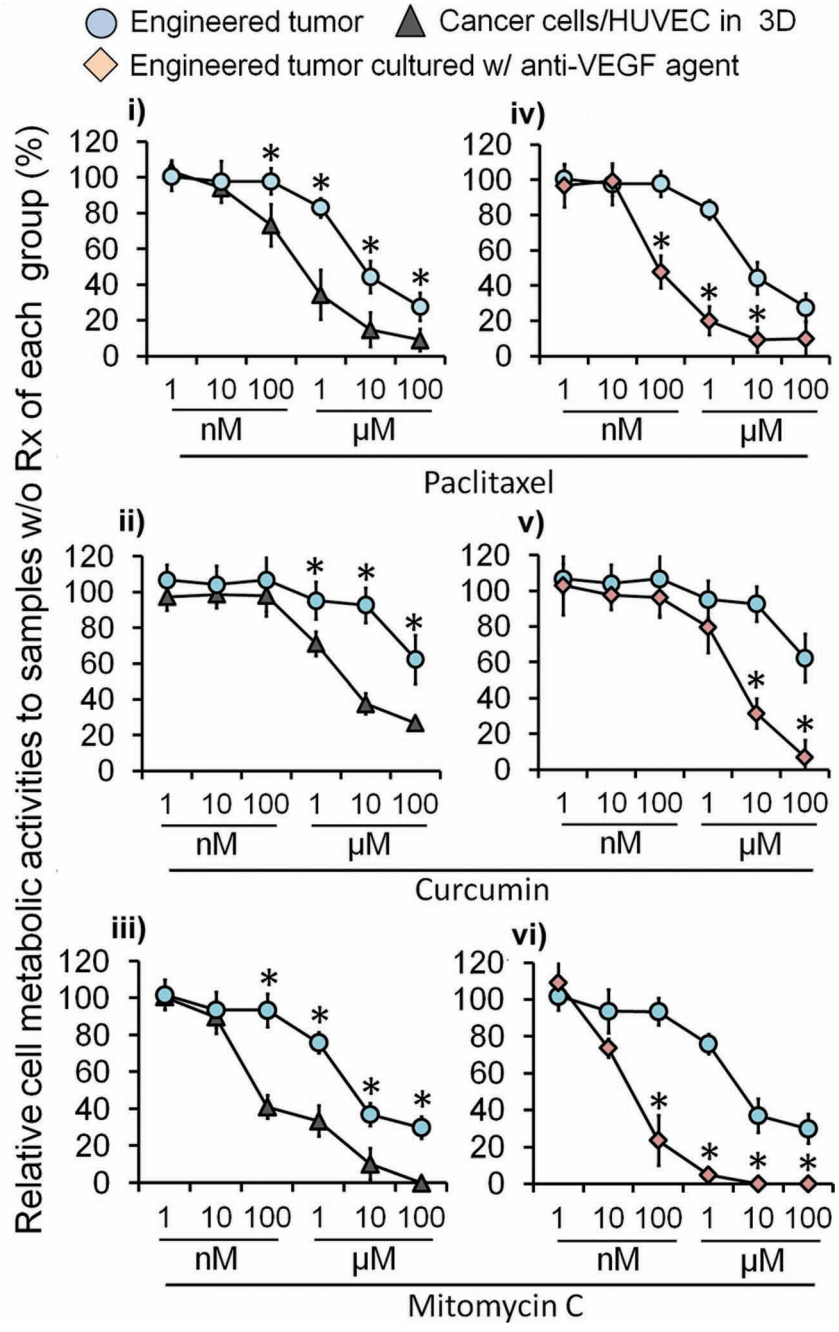

Figure 4. The metabolic activities of the same number of cancer cells and HUVEC in response to various chemotherapy drugs in different environments: coencapsulated into 3D hydrogel matrices with HUVEC without any pattern ('Cancer cells/HUVEC in 3D'), incorporated into the engineered tumors, and cultured with anti-VEGF agents in culture medium ('Engineered tumor cultured w/anti-VEGF agent'). The ratio of the number of cancer cells to HUVEC was 10:1. Statistical significance is denoted with asterisks when $p < 0.01$ ($n = 3$).

(750 μm). The hepatocytes were added to the hydrogel prepolymer at a concentration of 20×10^6 cells/mL. One of the cured matrices with hepatocytes was loaded in the center of the 2 mm diameter hole of a PDMS film with a thickness of 2 mm on a glass slide. 2 μL of hydrogel prepolymer with hepatocytes were loaded around the cured hydrogel matrix with HUVEC and the plate structure with HUVEC was stacked on them. Then, two more hydrogel prepolymer layers were deposited while another plate structure was inserted between them. In order to improve the permeability of the engineered liver lobule, we incorporated PLGA nanoparticles into the hydrogel matrix at 0.1% (w/v). We prepared the nanoparticles by dissolving PLGA into DCM and emulsifying the solution in water.[14] The layered prepolymer solution was covered by another glass slide and incubated at 37°C with 5% CO_2 for 30 min. The cured engineered liver lobules were subsequently washed with PBS and then cultured in ultralow attachment multiwell plates with hepatocyte cell-culture medium. The viability of the encapsulated hepatocytes was determined by counting live and dead cells manually (Live/Dead® assay, Invitrogen). The engineered liver lobules were cultured in hepatocyte culture media (Additional Materials and Methods in the Supporting Information).

To establish the spatial mimic of the initial phase of a cancer tumor, we stacked the L-shaped plate structure with HUVEC between two layers of 10 μL of the plain hydrogel prepolymer without cells. Approximately 1×10^4 cancer cells were placed at the designated distance from the plate structure. For the reconstruction of the highly vascularized mature tumor, the prepolymer with 40×10^6 cancer cells/mL was used. The engineered tumors were cultured in HUVEC culture medium (Additional Materials and Methods in the Supporting Information).

To obtain fluorescent images of the engineered tissues (Figure 2 and Figure 3), we prestained the cells in the hydrogel matrices (i.e., hepatocytes or cancer cells) red with DiI (Molecular Probes), and the cells on the plate structures (i.e., HUVEC) green with DiO (Molecular Probes) before constructing the tissue structures. Then we took multiple subfigures of the structures and assembled them into one figure. For the engineered liver lobule, the image of each layer of the engineered tissue was taken before it was stacked into the 3D structure for clear visibility.

Supporting Information

Supporting Information is available from the Wiley Online Library or from the author.

Acknowledgements

The authors acknowledge the Joseph and Sharon Saunders Fund for supporting this work. The authors are also grateful to Professor Gary K. Steinberg (Stanford University) for arranging the collaboration, Curtis W. Frank (Stanford University) for useful discussion, Professor Theo D. Palmer (Stanford University), Professor Lawrence Recht (Stanford University), and Professor Jeffrey S. Glen (Stanford University) for providing their lab facilities and materials for this work, and Dr. Hyejean Suh for helpful comments and suggestions for the manuscript.

Received: February 17, 2012
Revised: June 9, 2012
Published onine: August 24, 2012

[1] M. P. Lutolf, *Nat. Mater.* **2009**, *8*, 451.
[2] a) D. Huh, Y. Torisawa, G. A. Hamilton, H. J. Kim, D. E. Ingber, *Lab Chip* **2012**, *12*, 2156; b) I. K. Zervantonakis, C. R. Kothapalli, S. Chung, R. Sudo, R. D. Kamm, *Biomicrofluidics* **2011**, *5*, 013406.
[3] R. Gauvin, R. Parenteau Bareil, M. R. Dokmeci, W. D. Merryman, A. Khademhosseini, *Wiley Interdisciplinary Rev.: Nanomed. Nanobiotechnol.* **2011**, *4*, 235.
[4] a) A. M. Kloxin, A. M. Kasko, C. N. Salinas, K. S. Anseth, *Science* **2009**, *324*, 59; b) Y. Luo, M. S. Shoichet, *Nat. Mater.* **2004**, *3*, 249.
[5] a) D. R. Albrecht, G. H. Underhill, T. B. Wassermann, R. L. Sah, S. N. Bhatia, *Nat. Methods* **2006**, *3*, 369; b) C. T. Ho, R. Z. Lin, W. Y. Chang, H. Y. Chang, C. H. Liu, *Lab Chip* **2006**, *6*, 724.
[6] S. J. Hollister, *Nat. Mater.* **2005**, *4*, 518.
[7] R. Langer, J. P. Vacanti, *Science* **1993**, *260*, 920.
[8] M. C. Cushing, K. S. Anseth, *Science* **2007**, *316*, 1133.
[9] L. M. Sherwood, E. E. Parris, J. Folkman, *New England J. Med.* **1971**, *285*, 1182.
[10] D. Wirtz, K. Konstantopoulos, P. C. Searson, *Nat. Rev. Cancer* **2011**, *11*, 512.
[11] R. S. Kerbel, B. A. Kamen, *Nat. Rev. Cancer* **2004**, *4*, 423.
[12] R. K. Jain, *Nat. Med.* **2003**, *9*, 685.
[13] W. Lee, M. E. Wiseman, N. J. Cho, J. S. Glenn, C. W. Frank, *Biomaterials* **2009**, *30*, 6648.
[14] W. Lee, N.-J. Cho, A. Xiong, M. Elazr, J. S. Glenn, C. W. Frank, *Proc. Natl. Acad. Sci. USA* **2010**, *107*, 20709.
[15] N. Ferrara, R. S. Kerbel, *Nature* **2005**, *438*, 967.
[16] P. Carmeliet, R. K. Jain, *Nature* **2011**, *473*, 298.
[17] D. Hanahan, *Cell* **2000**, *100*, 57.
[18] L. Holmgren, M. S. O'Reilly, J. Folkman, *Nat. Med.* **1995**, *1*, 149.
[19] P. Carmeliet, R. K. Jain, *Nature* **2000**, *407*, 249.
[20] M. P. Lutolf, J. A. Hubbell, *Nat. Biotechnol.* **2005**, *23*, 47.